Available online at www.sciencedirect.com
SCIENCE DIRECT®
Journal of Asian Earth Sciences 23 (2004) 745–759
Journal of Asian Earth Sciences
www.elsevier.com/locate/jseaes

Geochemical signatures for eclogite protolith from the Maksyutov Complex, South Urals

N.I. Volkova*, A.E. Frenkel, V.I. Budanov, G.G. Lepezin

Institute of Mineralogy and Petrography, Russian Academy of Sciences, Pr. Koptyuga, 3, Novosibirsk 630090, Russia

Abstract

We conducted a geochemical study of eclogites (40 samples) from a boudin of the Lower Unit of the Maksyutov Complex in the South Urals in order to determine their protolith nature. The eclogites have major element compositions corresponding to quartz-bearing hypersthene basalts. Trace-element characteristics of the eclogites further suggest that they resemble enriched-type of tholeiites such as E-MORB. The compositional variation of eclogites was likely caused by fractional crystallization of parental melt under hypabyssal conditions, during its intrusion in thinned continental crust shortly before subduction. The high-pressure metamorphism has not affected significantly the major- and trace-element signatures of the protoliths. The compositions of co-existing minerals from the distinguished rock groups do not show significant distinctions. The considerable scatter of P–T estimates of metamorphic conditions does not depend on whole-rock composition. Therefore, the eclogitization was preceded by a chemical differentiation of an initial magmatic source, which is responsible for co-existence of rocks of variable composition in the same boudin. Dikes or sills of tholeiite basalts having geochemical characteristics of E-MORB could be the protoliths for the Maksyutov eclogites.

Keywords: Eclogite; Prodith; Maksyutov Complex

1. Introduction

The Maksyutov high-pressure metamorphic complex in the South Urals is one of the familiar eclogite localities. Its geological setting, complicated inner structure, age and PT conditions of metamorphism have been widely discussed (e.g. Dobretsov, 1974, 1991; Lennykh, 1977; Matte et al., 1993; Beane et al., 1995; Lennykh et al., 1995; Dobretsov et al., 1996; Chemenda et al., 1997; Echtler and Hetzel, 1997; Puchkov, 1997; Shatsky et al., 1997; Hetzel et al., 1998; Krasnobaev et al., 1998; Schulte and Blümel, 1999; Leech and Ernst, 2000; Beane and Connely, 2000; Glodny et al., 2002; Schulte and Sindern, 2002).

In the Maksyutov Complex eclogites occur as boudins within metasedimentary garnet–mica schists. The sedimentary protolith of the complex is considered to be an eastern margin of the East European platform, which was subducted beneath island arc (Leech and Ernst, 2000). It was supposed that an early extension along the eastern edge of the platform likely resulted in the shallow intrusion of mafic sills or dikes within the sedimentary section (Puchkov, 1997; Brown and Spadea, 1999; Leech and Ernst, 2000). The geochemical characteristics of the eclogites from the Maksyutov Complex and the pre-metamorphic history of their protoliths have remained practically unknown. Two recent studies have shown that the eclogites from the Maksyutov Complex correspond in composition to tholeiite basalts and have a MORB-type affinity (Schulte and Blümel, 1999; Leech and Ernst, 2000). But this conclusion was based mainly on bulk-rock composition data, including a limited number of analyses. To address this deficiency, we undertook a detailed geochemical study of eclogites from a boudin within the Maksyutov Complex. In this paper, the geochemistry and mineralogy of the eclogites are presented, and these data are integrated with previous studies of our group (Volkova et al., 2001) to discuss the origin of these eclogites.

2. Geological setting

The high-pressure Maksyutov Complex in the South Urals is located between the East European Platform and the Siberian Craton. It extends for 200 km N–S from head Sakmara River in the north to Guberly River in the south and forms a narrow belt of width 10–15 km (Fig. 1). It is

* Corresponding author.
E-mail address: nvolkova@uiggm.nsc.ru (N.I. Volkova).

1367-9120/03/$ - see front matter © 2003 Elsevier Ltd. All rights reserved.
doi:10.1016/S1367-9120(03)00128-7

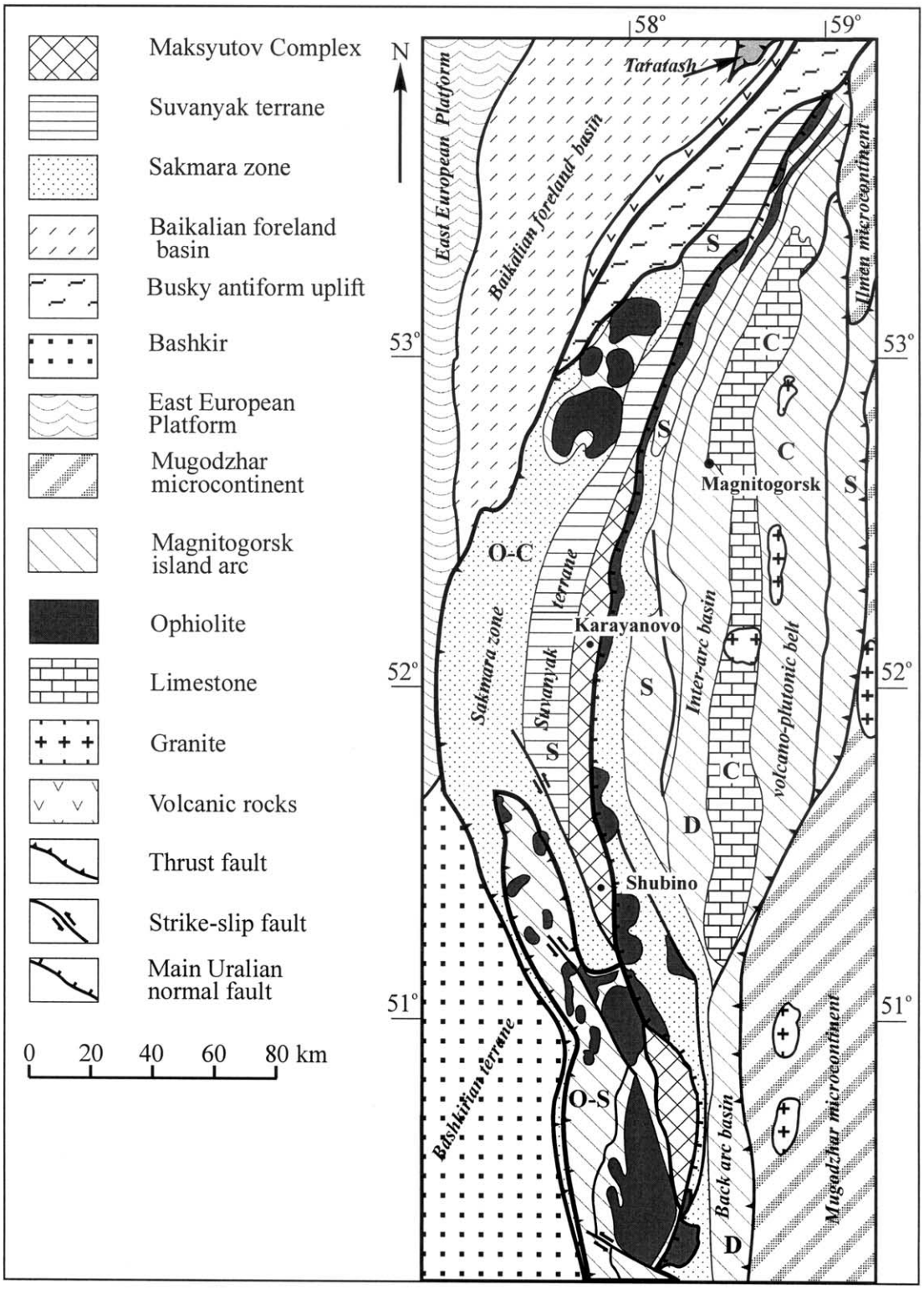

Fig. 1. Simplified geotectonic map of the Central Ural Mountains, showing the location of the Maksyutov Complex (after Lennykh et al., 1995; Dobretsov et al., 1996).

bordered on the east by Upper Ordovician–Silurian ophiolites and Devonian volcanic rocks of the Magnitogorsk island arc along the Main Uralian Normal Fault, which is regarded as the main suture zone of the Uralian orogenic belt. On the west it is tectonically juxtaposed with Lower Paleozoic platform sediments of the Suvanyak Complex and the Sakmara zone (Lennykh et al., 1995). The Maksyutov Complex originated as a result of Devonian subduction and

collision of the continental units of the East European Platform with the Devonian Magnitogorsk island arc (Schulte and Sindern, 2002).

The complex is divided into two tectonometamorphic units (Dobretsov, 1974, 1991; Lennykh et al., 1995). The structurally lower, eclogite-facies, Unit #1 is composed primarily of intensively sheared graphitic quartzites, mica and garnet–mica schists containing lenses and boudins of eclogites, coarse-grained blueschists, and rare bodies of olivine–enstatite, enstatite and quartz–almandine–jadeite rocks. Metasedimentary host rocks are interpreted as mainly Proterozoic upper continental crust of the East European passive margin (Dobretsov et al., 1996). Protolith ages for this unit are estimated between 800 and 1830 Ma, based on Rb/Sr whole rock data, and U/Pb zircon data (Dobretsov, 1974; Dobretsov et al., 1996).

All rocks from the Unit #1 of the Maksyutov Complex underwent multistage deformation and metamorphic recrystallization (Beane et al., 1995; Lennykh et al., 1995; Dobretsov et al., 1996; Hetzel et al., 1998; Schulte and Blümel, 1999). At least three stages of metamorphism and deformations are distinguished for the rocks from the Unit #1 rocks: 1-eclogite (garnet + omphacite + phengite + rutile), 2-blueschist (garnet + glaucophane + lawsonite + phengite), 3-greenschist (epidote + chlorite + albite + actinolite + muscovite). It is considered that blueschist/greenschist metamorphism was later and superimposed on mineral parageneses of eclogites (Schulte and Blümel, 1999; Leech and Ernst, 2000).

The age of the high-pressure metamorphism in the Unit #1 of the Maksyutov Complex is estimated to be 384 ± 4 and 377 ± 2 Ma, based on the U/Pb data on rutile (Beane and Connely, 2000). The published Sm/Nd isochrons yield age values between 399 ± 35 and 357 ± 15 Ma, with initial $^{143}Nd/^{144}Nd$ varying from 0.51207 ± 12 to 0.51253 ± 3 (Shatsky et al., 1997; Beane and Connely, 2000). In addition, $^{40}Ar/^{39}Ar$ data on phengite were reported for the Unit #1: 372 ± 4 to 388 ± 4 Ma (Matte et al., 1993; Lennykh et al., 1995). But these data were interpreted in a different way in the context of $P–T–t$ trend of tectonometamorphic evolution, including collision, subduction and an early stage of the exhumation history (Matte et al., 1993; Lennykh et al., 1995; Dobretsov et al., 1996; Echtler and Hetzel, 1997; Chemenda et al., 1997; Brown et al., 1998, 2000; Brown and Spadea, 1999; Hetzel et al., 1998; Beane and Connely, 2000; Leech and Ernst, 2000). Glodny et al. (2002) presented new, high-precision internal mineral Rb/Sr isochrons, mainly controlled by omphacite and phengite, which give concordant ages with an average value of 375 ± 2 Ma (2σ). These ages are regarded to reflect crystallization ages, related to the prograde eclogitization reactions.

Common mineral assemblages of eclogites and quartz–almandine–jadeite rocks indicate metamorphic temperatures of 550–650 °C and pressures of 15–23 kbar (Beane et al., 1995; Lennykh et al., 1995; Dobretsov et al., 1996; Hetzel et al., 1998; Schulte and Blümel, 1999). Reports of coesite and coesite pseudomorphs (Chesnokov and Popov, 1965; Dobretsov and Dobretsova, 1988), as well as unusual cuboid graphite aggregates considered as probable diamond pseudomorphs (Leech and Ernst, 1998) suggest that the pressures during an early stage of UHP metamorphism may have been greater than 25–27 and 32 kbar, respectively. But Glodny et al. (2002) showed that the possible occurrence of an earlier (pre-375 Ma) ultra-high-pressure metamorphism in the Maksyutov Complex is disproved by isotope systematics, microtextures, and mineral zoning patterns.

The upper Unit #2 is considered to be metaophiolite melange, composed of lenses and blocks of serpentinites, metabasalts, metagabbro and marbles in a recrystallized matrix of metagraywackes and graphite-bearing schists (Dobretsov, 1991; Dobretsov et al., 1996). The serpentinite melanges contain lawsonite-bearing metarodingites (Schulte and Sindern, 2002). Metabasites of the Unit #1 and the Unit #2 differ markedly in chemical and mineral composition (Lennykh et al., 1995; Dobretsov et al., 1996). P–T conditions of metamorphism of the Unit #2 rocks corresponded to transitional blueschist/greenschist facies and were estimated to be $T = 300–400$ °C and $P = 6–8$ kbar.

The Unit #1 and Unit #2 were tectonically juxtaposed after high-pressure metamorphism in the Unit #1, during retrograde metamorphism along a top-to the ENE shear zone (Hetzel, 1999) that yielded an Ar–Ar age of 365–355 Ma (Beane and Connely, 2000).

3. Eclogite boudin and analytical methods

A 5 × 30 m eclogite boudin examined in this study is exposed within sheared quartz–albite–mica schists on the east bank of Sakmara River at 2.5 km to the south from the Karayanovo village. The boudin appears banded due to thin alternation of green-colored omphacite-rich layers and black-colored glaucophane-rich layers. Hereafter they are referred to eclogites and glaucophane eclogites, respectively. These rocks have similar mineral paragenesis (amphibole + omphacite + garnet + quartz + phengite + zoisite (epidote) ± actinolite + rutile + titanite), but vary in proportions of the principal phases. Foliation is defined by omphacite, amphibole, zoisite and mica. Euhedral porphyroblasts of garnet are relatively coarse-grained (0.05–0.8 cm) and are scattered in a fine-grained matrix. Inclusions in garnet are quartz, phengite, amphibole, rutile.

We carried out a detailed sampling along the profile across the boudin extension. The collection includes 40 small, lithologically homogeneous samples of ~500 g. The chemical rock compositions of 40 samples of eclogite were obtained by X-ray fluorescence spectroscopy (XRF) by X-ray analyzer VRA-20 R. Losses on ignition were determined

by standard chemical method. For the majority of rock-forming components the detection limits were at a level of 0.02–0.005%, and only for MgO and Na_2O were equal to 0.1 and 0.2%, respectively. Rb, Sr, Nb, Zr, and Y were analyzed in 8 samples by energy-dispersive XRF with an accuracy of 5–10% and precision of 1–2%. Cs, Hf, Ta, U, Th, Cr, Co, Sc, REE contents were determined in the same samples by instrumental neutron-activation analysis with an accuracy of 5–10% and the following detection limits (in ppm): Cr: 10, Ce: 2, La, Co: 0.5, Cs, Th: 0.3, Sc, Sm: 0.2, U, Hf: 0.1, Eu, Lu, Nd: 0.05, Gd, Yb: 0.03, Tb, Ta: 0.02. The mineral compositions were determined using microprobe analyzer 'Camebax-Micro'. An accelerating potential of 20 kV, a beam current of 40 nA, counting time of 10 s, and a beam diameter of 2–3 μm were employed for most analyses. Natural and synthetic standards were used and the data were processed by the PAP routine. Analytical error for all components was less than 2%. All analyses were performed in the United Institute of Geology, Geophysics and Mineralogy, Novosibirsk, Russia.

4. Bulk-rock chemistry

The bulk chemistry of eclogites and glaucophane eclogites from the boudin, as may be deduced from the 40 analyses (Table 1), are comparable with basalts, with SiO_2 content varying from 47 up to 54 wt%. Only a few samples correspond to basaltic andesites. Maximum variations are noted for contents of alkali and alkaline-earth elements (MgO: 4.0–12.7 wt%; CaO: 4.7–13.6 wt%; Na_2O: 1.3–3.5 wt%; K_2O: 0.2–3.0 wt%).

Table 1
Whole-rock compositions of eclogites from the Maksyutov Complex

Sample no.	Rock	SiO_2	TiO_2	Al_2O_3	Fe_2O_3[a]	MnO	MgO	CaO	Na_2O	K_2O	P_2O_5	LOI	Total
1	Gln eclogite	49.91	1.53	12.34	12.77	0.17	12.44	6.72	1.87	0.39	0.15	1.71	100.00
2	Gln eclogite	49.65	1.89	15.32	13.45	0.16	7.65	5.52	2.86	1.23	0.21	2.07	100.02
3	Gln eclogite	50.88	1.60	11.65	12.35	0.15	12.18	6.19	2.74	0.41	0.10	1.83	100.09
4	Gln eclogite	51.85	1.23	12.61	12.63	0.20	11.48	6.05	1.91	0.35	0.14	1.54	99.99
5-2	Gln eclogite	46.54	1.00	11.82	12.51	0.18	13.30	8.00	2.00	0.40	0.17	4.16	100.08
8	Eclogite	50.88	1.42	14.39	12.59	0.16	8.61	6.10	1.71	1.65	0.28	2.24	100.02
9	Gln eclogite	51.75	1.44	15.30	12.46	0.16	8.55	4.64	2.28	1.38	0.20	1.90	100.05
10	Gln eclogite	49.45	1.32	18.01	10.48	0.14	5.77	6.16	3.13	2.96	0.31	2.23	99.97
11	Gln eclogite	49.50	1.49	15.12	12.96	0.16	8.89	4.81	3.18	1.45	0.21	2.22	99.98
12	Gln eclogite	48.66	1.72	15.28	13.48	0.17	9.01	4.55	3.14	1.44	0.14	2.45	100.04
13	Eclogite	49.85	1.48	15.34	12.41	0.17	8.06	6.49	3.18	0.83	0.34	1.89	100.03
14	Eclogite	47.63	1.61	17.31	12.94	0.17	7.88	6.06	2.45	2.12	0.21	1.66	100.04
15	Eclogite	49.11	1.53	17.07	11.74	0.16	6.58	6.19	2.40	2.52	0.24	2.55	100.09
18-1	Gln eclogite	48.50	1.87	16.05	13.30	0.17	7.81	6.20	3.09	1.44	0.19	1.44	100.05
18-2	Eclogite	47.94	1.71	17.00	11.72	0.17	6.60	7.63	3.03	2.10	0.21	1.95	100.04
19	Eclogite	47.34	1.84	16.49	12.91	0.16	7.95	6.27	3.04	1.77	0.14	2.01	99.97
20	Gln eclogite	48.50	1.98	15.88	13.19	0.18	7.82	6.54	2.87	1.35	0.17	1.52	99.99
21-1	Eclogite	51.42	1.73	14.88	12.34	0.17	7.32	6.56	2.87	1.15	0.14	1.38	99.97
21-2	Gln eclogite	48.96	2.12	15.09	13.88	0.18	8.55	6.49	2.59	0.80	0.15	1.18	99.99
21-3	Eclogite	48.91	1.72	16.27	12.12	0.15	6.99	6.84	3.00	1.90	0.18	2.00	100.09
22-1	Gln eclogite	46.54	0.89	18.31	11.54	0.16	4.72	13.27	1.57	0.38	0.22	2.39	99.99
22-2	Eclogite	54.03	1.55	13.57	12.19	0.16	6.82	7.33	2.41	0.18	0.18	1.62	100.06
23-1	Gln eclogite	53.94	1.19	15.61	10.75	0.17	4.01	9.77	1.35	0.87	0.24	2.21	100.10
23-2	Gln eclogite	53.37	1.15	16.26	10.43	0.17	3.98	10.90	1.29	0.58	0.22	1.61	99.97
24	Eclogite	49.08	1.91	17.37	12.08	0.17	5.48	8.52	1.78	1.47	0.21	1.96	100.03
25	Eclogite	48.11	1.89	16.46	12.16	0.16	6.47	8.14	3.23	1.45	0.19	1.77	100.03
26	Gln eclogite	49.09	1.36	17.05	11.37	0.16	6.06	9.65	2.13	0.83	0.15	2.17	100.02
27	Eclogite	50.51	1.40	15.97	12.22	0.17	5.93	9.33	2.08	0.44	0.15	1.82	100.01
28	Eclogite	49.11	1.52	17.71	11.12	0.15	6.45	6.17	2.44	2.32	0.25	2.86	100.10
29	Eclogite	48.36	1.93	16.33	12.70	0.16	7.53	5.97	3.49	1.55	0.12	1.92	100.06
30	Gln eclogite	48.77	1.96	15.36	13.80	0.18	8.66	5.17	3.02	0.96	0.29	1.85	100.00
31	Eclogite	49.93	1.71	15.73	12.76	0.17	7.27	7.48	2.37	0.82	0.27	1.59	100.09
32-1	Eclogite	49.04	1.37	18.02	10.76	0.15	5.58	6.38	3.10	3.08	0.34	2.20	100.02
32-2	Eclogite	52.20	1.38	11.50	12.28	0.16	11.39	5.27	2.02	0.50	0.11	3.15	99.96
33-1	Gln eclogite	49.04	1.54	15.05	13.58	0.15	8.68	5.49	2.45	1.69	0.18	2.21	100.06
33-2	Gln eclogite	48.67	1.64	15.58	13.31	0.17	8.69	4.94	2.81	1.59	0.17	2.44	100.02
34	Gln eclogite	49.69	1.78	15.04	13.26	0.16	8.48	5.21	2.89	1.45	0.23	1.80	99.90
35	Gln eclogite	50.51	1.00	16.23	11.23	0.16	5.64	10.15	2.23	0.45	0.16	2.33	100.10
36	Gln eclogite	48.19	1.41	18.12	10.88	0.15	6.40	7.46	2.65	2.26	0.19	2.32	100.04
37	Gln eclogite	47.37	1.45	17.29	11.84	0.16	6.42	8.75	2.58	1.28	0.21	2.65	99.99

[a] $Fe_2O_3 + 1.11FeO$.

Table 2
Statistical comparison of major oxide contents in eclogites and glaucophane eclogites, using the Student's *t*-criterion and the Fisher's *F*-criterion

Statistical parameters	SiO_2	TiO_2	Al_2O_3	$Fe_2O_{3(tot)}$	MnO	MgO	CaO	Na_2O	K_2O	P_2O_5	LOI
Eclogite, $n = 16$											
Average	49.87	1.61	15.87	12.12	0.16	7.13	7.11	2.53	1.41	0.20	2.02
Stand. deviation	2.03	0.22	1.62	0.64	0.01	1.60	1.48	0.63	0.72	0.06	0.47
Glaucophane eclogite, $n = 24$											
Average	49.37	1.52	15.49	12.44	0.17	8.09	6.90	2.53	1.22	0.20	2.10
Stand. deviation	1.64	0.33	1.88	1.07	0.01	2.41	2.12	0.52	0.75	0.06	0.58
t, $t_{05} = 1.68$	0.78	0.97	0.64	1.10	0.00	1.41	1.99	0.00	0.76	0.21	0.45
F, $F_{05} = 2.13$	0.65	0.47	1.35	0.36	0.29	0.44	0.48	0.69	0.93	0.91	0.66

The statistical comparison of bulk compositions of eclogites and glaucophane eclogites showed the lack of significant distinctions between them at 95% significance level (Table 2). The similarity of these rocks suggests the isochemical behavior of major elements during high-pressure metamorphism and retrogressive stages (Volkova et al., 2001).

But when we used the cluster analysis, the three rock groups were distinguished (Table 3). These groups (termed as *clusters*) display statistical discrepancies in their chemical compositions. As eclogite and glaucophane eclogite samples fell into the all three clusters (for example, ratios of eclogites and glaucophane eclogites in the largest clusters I and II are 43 and 57%, 47 and 53%, accordingly), we conclude that the established geochemical discrimination has not resulted from metamorphic differentiation, but is due to initial distinctions of protolith compositions.

The cluster I ($n = 21$) comprises rocks with increased contents of MgO, TiO_2, ($FeO + Fe_2O_3$) and decreased contents of CaO and Al_2O_3 as compared with rocks of the cluster II ($n = 14$), which, on the contrary, are richer in alumina and calcium oxides. The cluster III consists only of five samples, bearing similarities in chemical composition with the rocks of the cluster I (increased contents of mafic components), but differs from them by considerably higher contents of MgO and sharply depleted concentrations of Al_2O_3, K_2O, and P_2O_5.

The established distinctions of the rock chemistry are embodied in CIPW normative rock compositions (Table 3). The rocks of the cluster II are characterized by higher contents of normative plagioclase and clinopyroxene and by correspondingly lower contents of normative orthopyroxene as compared to rocks of the cluster I. The rocks with the highest content of hypersthene and the lowest content of plagioclase fall into the cluster III. As a whole, the normative compositions of the majority of the analyzed eclogites suggest that their protoliths can be quartz-bearing hypersthene basalts of tholeiite series.

The distinctions in major element contents between the rocks of the distinguished clusters are clearly seen on the plots of major element oxides vs. MgO (Fig. 2). One can observe a continuous variation trend of rock compositions for clusters I and II and an isolated position of figurative points for cluster III rocks. The results of correlation analysis point to high degrees of correlation between MgO and $FeO + Fe_2O_3$ ($r = +0.86$), TiO_2 ($r = +0.9$), and significant inverse correlation between MgO and Al_2O_3 ($r = -0.56$) and CaO ($r = -0.83$) for the rocks relating to the first two clusters ($n = 35$; $r_{05} = 0.35$). The pronounced negative correlation between MgO and CaO suggests that clinopyroxene was not an important fractionating phase. The distinction of cluster III chemistry from the remainder eclogites, alongside with high Mg# values—MgO/($FeO + 0.9Fe_2O_3$) = 1.18–1.01 (for the rocks of clusters I and II they are 0.76–0.66 and 0.65–0.41, correspondingly),

Table 3
Average contents of major oxides (wt%) and their standard deviations in distinguished eclogite clusters and calculated CIPW norms for their magmatic protoliths

Oxide	I cluster ($n = 21$)	II cluster ($n = 14$)	III cluster ($n = 5$)
SiO_2	49.48 ± 1.52	49.45 ± 2.09	50.28 ± 2.27
TiO_2	1.71 ± 0.20	1.40 ± 0.30	1.35 ± 0.24
Al_2O_3	15.55 ± 0.86	17.10 ± 0.88	11.98 ± 0.47
Fe_2O_3[a]	12.92 ± 0.58	11.33 ± 0.62	12.51 ± 0.20
MnO	0.17 ± 0.01	0.16 ± 0.01	0.17 ± 0.02
MgO	7.99 ± 0.72	5.68 ± 0.88	12.16 ± 0.78
CaO	5.95 ± 0.84	8.73 ± 1.99	6.45 ± 1.01
Na_2O	2.77 ± 0.41	2.33 ± 0.66	2.11 ± 0.36
K_2O	1.39 ± 0.51	1.46 ± 0.94	0.41 ± 0.06
P_2O_5	0.20 ± 0.06	0.22 ± 0.05	0.13 ± 0.03
LOI	1.90 ± 0.37	2.18 ± 0.34	2.48 ± 1.14
Total	100.02	100.03	100.02
Pl	50.2	52.7	40.9
Opx	27.7	17.9	36.2
Cpx	1.9	8.3	7.4
Qtz	0.8	2.6	3.1
Ol	0.0	0.0	0.0
Or	8.4	8.8	2.5
Mat	6.4	5.6	6.2
Ilm	3.3	2.7	2.6
Ap	0.5	0.5	0.3
Crn	0.0	0.0	0.0

[a] $Fe_2O_3 + 1.11FeO$.

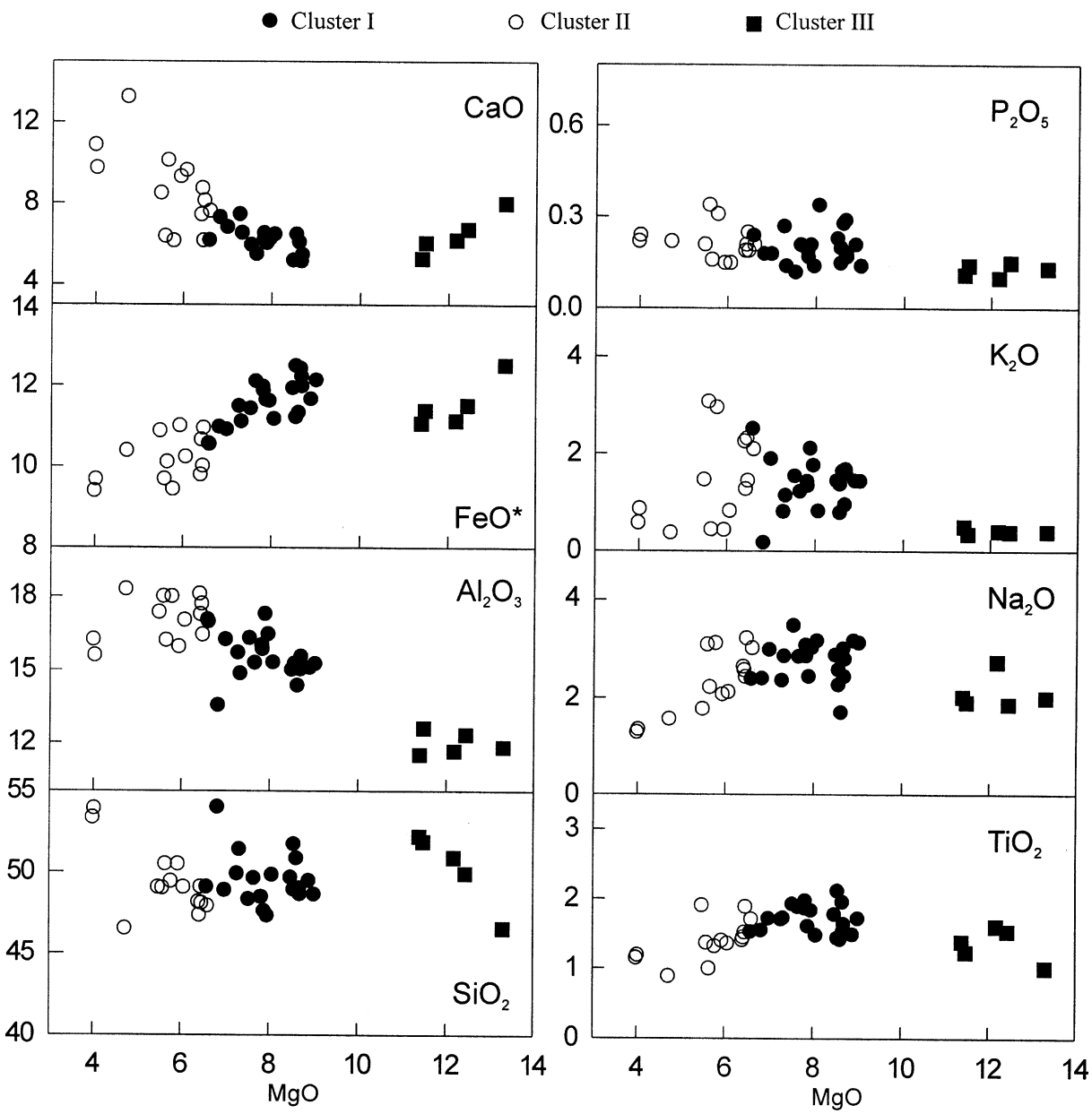

Fig. 2. Variations of major oxides vs. MgO for eclogites from the Maksyutov Complex. Total iron as FeO^*.

are suggestive of a cumulative nature of their protolith. Such cumulative process can take place in a sill or dyke of small thickness, but is highly improbable in a lava sheet.

5. Minor and trace elements

The behavior of trace elements is believed by many petrologists to be the best indicators both for determining the origin and for establishing the geodynamic settings of basaltic rocks, even when they have been subjected to high-grade metamorphism.

The inheritance of primary magmatic composition in eclogites and glaucophane eclogites is confirmed by a high positive linear correlation between contents of high-strength incompatible elements—Zr, Hf, Nb, Ta, Y, HREE, Ti (Table 4). The tholeiite nature of the rocks is also implied by discriminant diagrams TiO_2–Zr/P_2O_5, Zr–Zr/Y (Winchester and Floyd, 1976; Pearce and Norry, 1979), which permit to distinguish alkali and tholeiite basalts (here these plots are omitted).

In the triangular diagram Ti–Zr–Y (Pearce and Cann, 1973) eclogites of the Maksyutov Complex plot within the field of ocean-floor basalts (Fig. 3a). In the Th–Hf–Ta diagram (Wood, 1980) all the eclogite samples fall into the field of E-MORB (Fig. 3b). Only in the Zr–Nb–Y diagram (Meschede, 1986), the different clusters can be discriminated (Fig. 3c): the calcium-enriched cluster II rocks plot

Table 4
Trace element data (ppm) for representative eclogites from the Maksyutov Complex

	Cluster I			Cluster II				Cluster III
Sample no.	8	21-1	21-2	10	23-1	23-2	32-1	32-2
Rb	35.9	22.7	13.8	57.7	13.7	8.3	51.2	6.8
Cs	1.6	1.3	0.9	1.3	3.6	0.7	3.6	0.4
Sr	166	158	125	338	500	698	316	58
U	0.30	0.22	0.20	0.25	0.30	0.30	0.20	0.36
Th	0.8	0.44	0.52	0.40	0.50	0.35	0.50	0.46
Nb	10.8	10.0	9.9	4.8	2.9	2.4	3.7	10.3
Ta	0.40	0.40	0.50	0.25	0.32	0.26	0.33	0.34
Zr	83	88	101	70	89	79	90	84
Hf	2.3	2.2	3.2	1.7	1.9	1.6	2.1	1.9
La	9.7	8.9	11.2	7.7	9.5	10.0	11.7	7.9
Ce	16.0	15.0	23.8	13.8	17.5	13.0	23.4	11.4
Nd	11.8	11.0	14.3	10.7	11.5	12.0	13.2	9.8
Sm	3.2	3.0	3.9	3.0	3.1	3.5	3.4	2.9
Eu	1.30	1.10	1.37	1.20	1.39	1.40	1.40	0.98
Gd	3.6	3.3	4.5	3.5	3.4	4.3	3.7	3.9
Tb	0.60	0.56	0.76	0.61	0.57	0.70	0.62	0.68
Yb	1.79	1.69	2.37	2.03	1.67	2.04	1.72	2.02
Lu	0.26	0.24	0.34	0.30	0.24	0.29	0.25	0.29
Y	21.2	22.4	28.8	20.7	28.2	26.7	22.6	30.0
Sc	36.2	32.9	39.4	33.5	26.6	35.8	27.1	32.5
Co	44	42	51	26	32	26	32	51
Cr	164	270	230	112	94	90	95	540

within the field of N-MORB, and Mg-enriched rocks of clusters I and III are in the field of E-MORB.

Here we want to cite a statement by Piboule and Briand (1985), who noted that the using of geochemical diagrams for paleotectonic discrimination may sometimes lead to inconclusive, or even misleading results. Did these rocks occurring in the same boudin really formed under different geodynamic environments? We believe that the observed distinctions are likely to be a consequence of enrichment of residual melt as a result of fractional crystallization and cumulative processes. Recall that all these geochemical diagrams were constructed only for basalt lava sheets, not for small intrusive dikes or sills. The geochemical character of the studied rocks really relates to their mantle-source composition and evolution rather to their 'true' tectonic setting. The 'MORB affinity' of their igneous protoliths are only indicative of a spreading environment.

The eclogites show LREE-enriched patterns (Fig. 4), with $(La/Lu)_n$ ratio ranging from 2.7 to 4.8. As a whole, they are comparable to those of E-MORB (Thompson et al., 1989). However, the three rock clusters do not show any substantial difference in total REE contents, nor in their distribution patterns. Almost all rocks are characterized by negative Ce anomalies, the appearance of which are yet

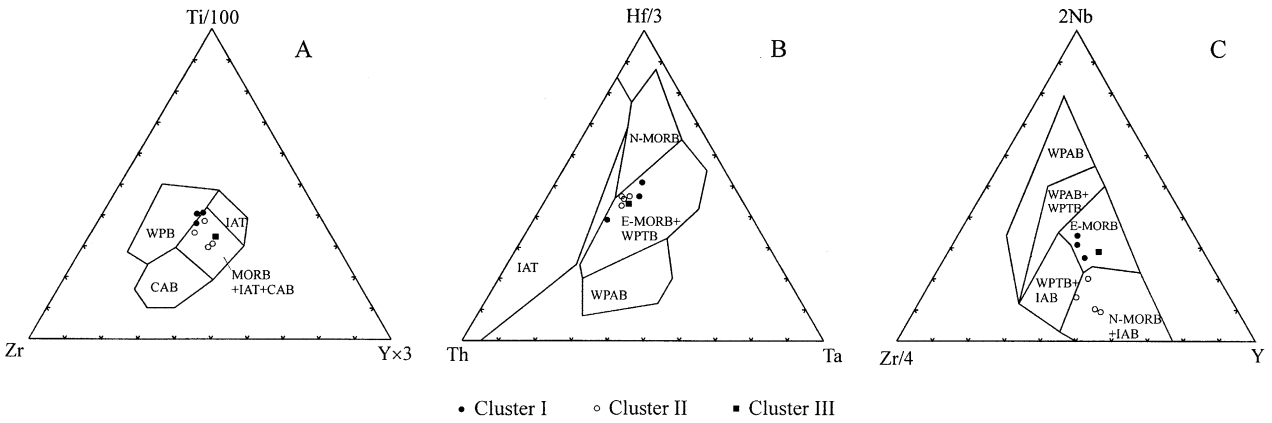

Fig. 3. Trace element distributions in the eclogites from the Maksyutov Complex. (A) Zr–Ti–Y plot with petrotectonic fields after Pearce and Cann (1973). (B) Th–Hf–Ta plot with fields from Wood (1980). (C) Zr–Nb–Y diagram with fields after Meschede (1986). CAB = calc-alkaline basalt; IAB = island arc basalt; IAT = island arc tholeiite; MORB = ocean-floor basalt; E-MORB = enriched type MORB; N-MORB = normal type MORB; WPB = within-plate basalt; WPAB = within-plate alkaline basalt; WPTB = within-plate tholeiite basalt.

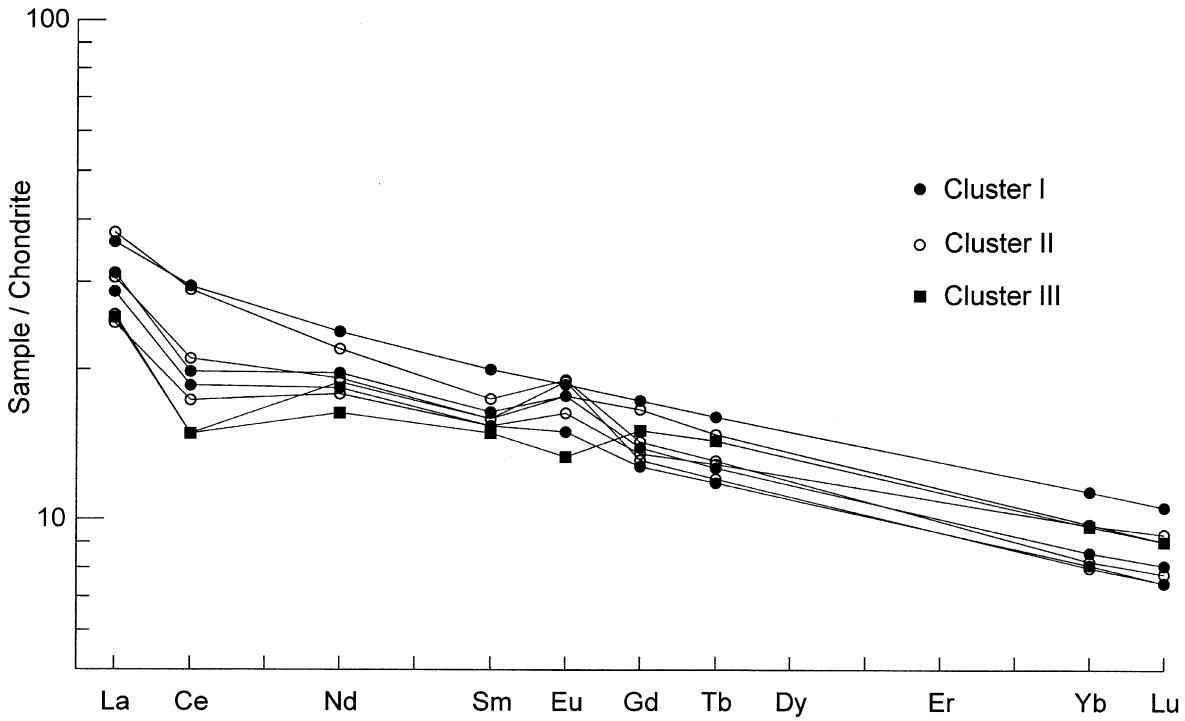

Fig. 4. Chondrite-normalized REE distribution patterns of eclogites from the Maksyutov Complex.

ambiguous, though Ce anomalies (positive and negative) are observed sometimes in REE patterns of individual eclogites from different regions (for example, Mottana et al., 1985; Piboule and Briand, 1985; Wang, 1998; Zhang et al., 2000; Xiao et al., 2001). We believe that this feature needs verification, because it can be an artifact.

The only difference between the distinguished rock clusters is a behavior of europium. In the REE patterns of Ca-enriched rocks (cluster II) there is a marked Eu-maximum due to plagioclase fractionation. For Mg-enriched rocks the different cases were noted: distinct or slightly appreciable maximum (samples 8 and 21-1, cluster I); lack of Eu-anomalies (sample 21-2, cluster I); and even the Eu-minimum, suggesting the intercumulus plagioclase crystallization (sample 32-2, cluster III).

The difference in trace-element characteristics between the rock clusters is clearly visible in the spidergrams (Fig. 5). Cluster II rocks show strong alkali (K, Rb, Cs) and Sr enrichments, but Nb depletion. This is usually noted for basalts formed in subduction environments. By contrast, eclogites of clusters I and III are characterized by more flattened patterns, and even a Sr-minimum is noted for sample 32-2 (cluster III). There are also minor distinctions between contents Ti, Hf and Ta in the distinguished rock clusters. As a whole, the eclogites show geochemical characteristics resembling basalts of E-type MORB. The only exception is the high contents of alkaline elements (K, Rb, Cs), which can be due to the peculiarities of magmatic source composition. Alternatively, crust contamination during intrusion, or mobility of alkalis in multi-stage processes of metamorphism, could also be the cause for alkali enrichments.

Thus, we can conclude that the processes of fractional crystallization result, on one hand, in plagioclase-rich rocks (II cluster), characterized by higher CaO and Al_2O_3 contents, as well as by the presence of Sr-maximum and Nb-minimum in the spidergram and Eu-minimum in the REE distribution pattern, and, on the other hand, in rocks with increased content of normative orthopyroxene. The last rocks have higher TiO_2, FeO_{tot}, MgO, Nb, Ta, Hf, Co, Cr values and lower concentrations of CaO, Al_2O_3, Sr (I cluster).

The third cluster rocks, the figurative points of which compositions occupy the isolated position away from common variation trends in practically all the geochemical plots, can be originated as a result of cumulative processes, which are not common for effusive flows, but can take place in sills or dikes, crystallized under hypabyssal conditions. The cumulative nature of these rocks is indicated by sharply decreased contents of Al_2O_3, K_2O, P_2O_5, Rb, Cs, Sr, REE and higher contents of MgO, Co, Cr as compared with the other rocks of the examined boudin (Tables 1 and 2), as well as by the presence of negative Eu-anomaly in the REE distribution pattern.

6. Mineral chemistry

In general, chemical compositions of metamorphic minerals record information on their physicochemical

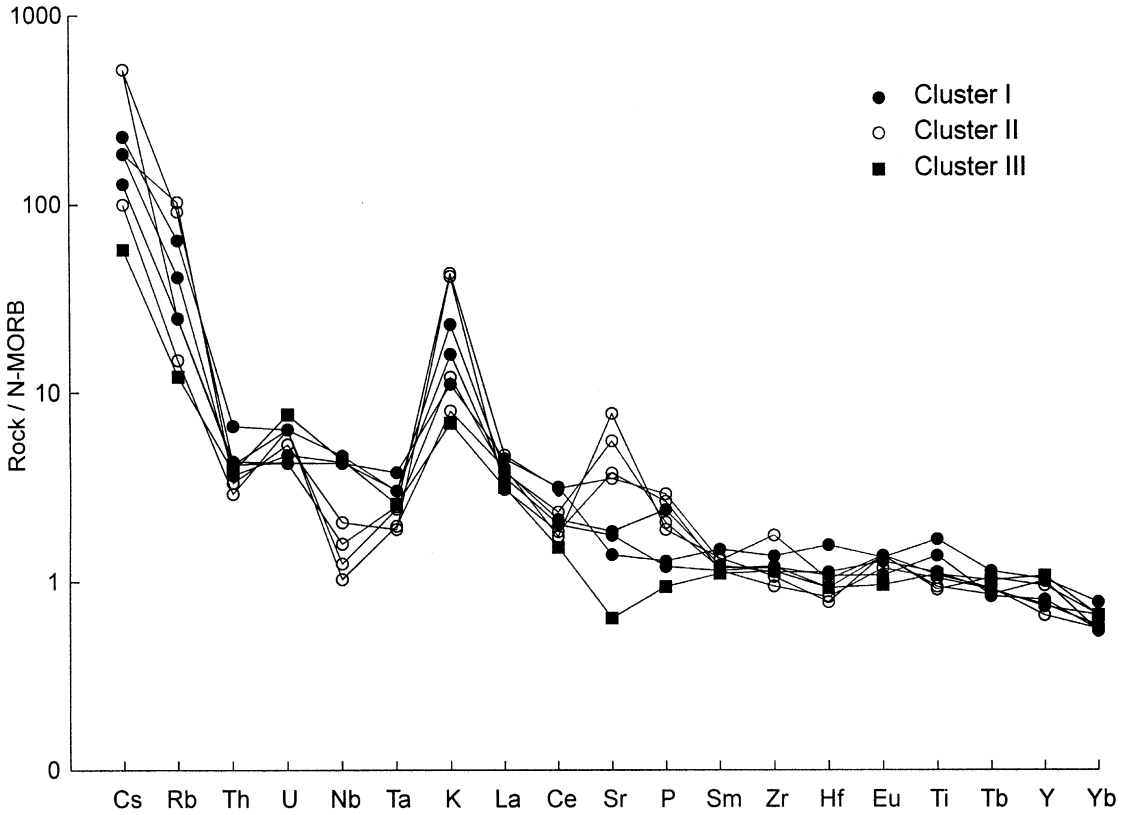

Fig. 5. Spidergrams of eclogites from the Maksyutov Complex.

formation conditions. However, the variation of mineral chemistry is also influenced by several other factors, including the whole-rock chemical composition and the coexisting mineral assemblage. We have attempted to clarify the influence of whole-rock composition on the constituent mineral chemical compositions.

The wide compositional range of garnets is shown in Table 5 and Fig. 6. Zonation of garnets reveals increasing Mg- and decreasing Ca-contents from cores toward rims. Also, iron content in most of the garnets decreases from core to rim, whereby some garnets show a relatively constant almandine content. Omphacite has a jadeite component between Jd_{43} and Jd_{50} and shows little variation in composition (Table 5, Fig. 7). Phengites contain appreciable amounts of celadonite component, with Si varying from 3.29 to 3.46 p.f.u. (Table 5). Large phengite crystals contain low Si in cores, while their rims as well as small phengite flakes are characterized by higher Si-concentrations.

Amphiboles from the analyzed rocks are glaucophane and barroisite (Table 5, Fig. 8). The observed glaucophane + barroisite amphibole assemblages probably represent non-equilibrium pairs (cf. Ernst, 1979), but now we cannot conclude the sodic amphibole either grew earlier or later than the barroisitic amphibole. In general, glaucophane grains vary in Ca and Mg content but do not exhibit any regular zoning pattern and commonly stay within the Na-amphibole range. Mg# number varying from 0.68 to 0.81 and $Fe^{3+}/(Fe^{3+} + Al^{VI})$ varying from 0.0 to 0.2. The Na_B content in barroisites is 0.96–1.15, $Mg/(Mg + Fe^{2+})$-ratio varies from 0.78 to 0.91.

Comparison of mineral chemistry from the distinguished rock clusters does not reveal any distinctions between them. Only compositions of garnet cores, omphacite cores, as well as glaucophanes exhibit some differences. Garnet cores from cluster II are rich in almandine, but poor in grossular, and are distinguishable from those of clusters I and III. However, garnet rims of all the clusters are comparable in composition. Omphacite from cluster II rocks is slightly enriched in jadeite component as compared to that of cluster I. Glaucophane from cluster II contains slightly more calcium in comparison with glaucophanes from clusters I and III. At first glance, the result seems paradoxical, because the cores of garnet and omphacite grains from cluster II rocks (enriched in CaO) are characterized by lower Ca content. We believe that this is due to different metamorphic responses of different protoliths to the changes in P–T conditions during subduction. The different reaction ways led to the slightly distinctions between chemical compositions of early mineral phases, now-presented by garnet and omphacite cores. Furthermore, this fact can be also explained by the higher contents of clinopyroxene in cluster II rocks.

Table 5
Representative analyses of major constituent minerals from the eclogite boudin, Maksyutov Complex (c = core; r = rim)

Sample no.	8 (Cluster I)				21/1 (Cluster I)						21/2 (Cluster I)				
Mineral	Gl	Grt-c	Grt-r	Phg	Gl	Grt-c	Grt-r	Omp	Phg	Ep	Bar	Gl	Grt-c	Grt-r	Phg
SiO_2	58.19	38.98	38.70	50.15	58.39	39.58	40.13	56.30	52.20	38.45	52.65	59.32	38.88	39.36	49.86
TiO_2	0.03	0.10	0.05	0.95	0.03	0.11	0.07	0.12	0.19	0.13	0.27	0.01	0.09	0.07	0.57
Al_2O_3	10.93	21.35	22.23	28.18	10.12	21.36	21.80	10.82	26.19	24.92	10.89	11.43	21.05	21.60	27.51
Cr_2O_3	0.09	0.09	0.05	0.11	0.02	0.00	0.00	0.03	0.04	0.01	0.00	0.01	0.00	0.01	0.06
FeO[a]	8.00	25.00	24.08	1.53	9.52	24.19	23.47	5.68	2.68	9.62	7.50	7.48	27.11	23.34	1.91
MnO	0.00	0.30	0.13	0.00	0.03	0.48	0.31	0.01	0.02	0.11	0.00	0.00	0.50	0.22	0.00
MgO	11.75	4.76	7.69	3.83	11.59	6.50	8.73	7.73	4.02	0.08	14.59	11.69	3.95	7.26	3.79
CaO	1.32	8.82	6.29	0.01	1.18	8.32	6.04	12.12	0.02	23.17	6.60	0.76	8.09	7.78	0.01
Na_2O	6.97	0.01	0.01	0.75	6.84	0.08	0.04	7.50	0.29	0.01	4.21	6.45	0.06	0.03	0.78
K_2O	0.02	0.01	0.01	9.53	0.02	0.02	0.02	0.03	10.40	0.02	0.33	0.01	0.00	0.01	9.78
Total	97.29	99.41	99.24	95.02	97.73	100.63	100.61	100.35	96.05	96.51	97.05	97.15	99.73	99.68	94.27
Si	7.93	3.06	2.99	3.33	7.94	3.04	3.05	1.99	3.45	3.04	7.31	7.99	3.07	3.03	3.35
Ti	0.00	0.01	0.00	0.05	0.00	0.01	0.00	0.00	0.01	0.01	0.03	0.00	0.01	0.00	0.03
Al	1.76	1.97	2.03	2.21	1.62	1.93	1.95	0.45	2.04	2.32	1.78	1.82	1.96	1.96	2.18
Fe^{2+}	0.78	1.64	1.56	0.05	0.74	1.55	1.49	0.10	0.13	0.04	0.47	0.55	1.78	1.50	0.09
Fe^{3+}	0.13	0.00	0.00	0.03	0.34	0.00	0.00	0.07	0.02	0.60	0.40	0.29	0.00	0.00	0.02
Mn	0.00	0.02	0.01	0.00	0.00	0.03	0.02	0.00	0.00	0.01	0.00	0.00	0.03	0.01	0.00
Mg	2.39	0.56	0.89	0.38	2.35	0.74	0.99	0.41	0.40	0.01	3.02	2.35	0.46	0.83	0.38
Ca	0.19	0.74	0.52	0.00	0.17	0.68	0.49	0.46	0.00	1.96	0.98	0.11	0.68	0.64	0.00
Na	1.84	0.00	0.00	0.10	1.80	0.00	0.00	0.51	0.04	0.00	1.13	1.68	0.00	0.00	0.10
K	0.00	0.00	0.00	0.81	0.00	0.00	0.00	0.00	0.88	0.00	0.06	0.00	0.00	0.00	0.84
Total	15.03	7.99	7.99	6.95	14.97	7.99	7.99	3.99	6.96	7.99	15.17	14.80	7.99	7.99	6.99

Sample no.	10 (Cluster II)					23/1 (Cluster II)					23/2 (Cluster II)				
Mineral	Bar	Gl	Grt-c	Grt-r	Phg	Gl	Grt-c	Grt-r	Omp	Phg	Gl	Grt	Grt	Omp	Phg
SiO_2	51.82	58.30	37.89	39.25	50.93	58.88	37.90	38.75	56.44	51.69	57.71	38.57	39.56	56.32	51.74
TiO_2	0.30	0.01	0.09	0.03	0.19	0.00	0.08	0.02	0.09	0.24	0.03	0.07	0.03	0.10	0.18
Al_2O_3	11.41	11.00	20.83	21.50	28.55	10.92	20.93	21.29	11.39	26.83	9.52	20.90	21.27	11.44	25.71
Cr_2O_3	0.04	0.02	0.02	0.04	0.05	0.03	0.03	0.06	0.04	0.04	0.00	0.00	0.04	0.00	0.00
FeO[a]	7.74	8.31	28.40	24.69	1.92	8.99	27.66	25.31	5.12	2.77	9.44	27.45	25.05	6.09	2.86
MnO	0.02	0.05	0.62	0.25	0.00	0.05	1.63	0.47	0.01	0.00	0.06	0.67	0.40	0.03	0.01
MgO	14.79	11.81	4.49	8.32	3.55	11.04	4.41	7.25	8.01	3.67	11.96	4.58	7.79	7.42	3.93
CaO	7.04	1.35	7.53	5.76	0.00	0.89	7.48	6.43	12.89	0.00	1.99	7.48	6.08	11.04	0.01
Na_2O	4.30	6.77	0.01	0.05	0.57	7.06	0.05	0.02	6.83	0.48	7.95	0.06	0.07	8.08	0.33
K_2O	0.46	0.01	0.00	0.00	10.03	0.02	0.00	0.00	0.00	10.84	0.02	0.01	0.01	0.00	10.31
Total	97.92	97.64	99.89	99.90	95.79	97.88	100.18	99.60	100.81	96.57	98.68	99.77	100.31	100.52	95.08
Si	7.16	7.91	2.99	3.02	3.36	7.99	2.98	3.01	1.99	3.42	7.92	3.03	3.04	1.98	3.46
Ti	0.03	0.00	0.01	0.00	0.01	0.00	0.00	0.00	0.00	0.01	0.00	0.00	0.00	0.00	0.01
Al	1.86	1.76	1.93	1.95	2.22	1.75	1.94	1.95	0.47	2.09	1.54	1.94	1.92	0.47	2.03
Fe^{2+}	0.46	0.69	1.78	1.56	0.09	0.87	1.71	1.60	0.15	0.15	1.08	1.80	1.60	0.08	0.15
Fe^{3+}	0.43	0.25	0.08	0.02	0.02	0.14	0.10	0.04	0.00	0.00	0.00	0.00	0.01	0.10	0.01
Mn	0.00	0.01	0.04	0.02	0.00	0.01	0.11	0.03	0.00	0.00	0.01	0.04	0.03	0.00	0.00
Mg	3.05	2.39	0.53	0.95	0.35	2.23	0.52	0.84	0.42	0.36	2.45	0.54	0.89	0.39	0.39
Ca	1.04	0.20	0.64	0.47	0.00	0.13	0.63	0.53	0.49	0.00	0.29	0.63	0.50	0.42	0.00
Na	1.15	1.78	0.00	0.00	0.07	1.86	0.00	0.00	0.47	0.06	2.11	0.00	0.00	0.55	0.04
K	0.08	0.00	0.00	0.00	0.85	0.00	0.00	0.00	0.00	0.92	0.00	0.00	0.00	0.00	0.88
Total	15.27	14.97	8.00	7.99	6.97	14.99	7.99	7.99	4.00	7.01	15.41	7.99	7.99	4.00	6.97

(*continued on next page*)

Table 5 (*continued*)

Sample no.	32/1 (Cluster II)					32/2 (Cluster III)			
Mineral	Gl	Grt-c	Grt-r	Omp	Phg	Gl	Grt-c	Grt-r	Phg
SiO_2	59.06	38.86	38.50	56.25	50.16	58.64	39.04	39.64	51.53
TiO_2	0.00	0.00	0.01	0.04	0.37	0.02	0.11	0.04	0.20
Al_2O_3	10.68	21.40	21.45	10.01	28.74	10.60	21.27	21.76	26.64
Cr_2O_3	0.01	0.02	0.02	0.01	0.01	0.00	0.01	0.01	0.00
FeO[a]	9.42	24.87	24.17	6.78	2.64	9.16	23.76	23.43	2.46
MnO	0.05	0.62	0.49	0.02	0.02	0.03	0.53	0.25	0.00
MgO	11.42	8.53	9.54	7.39	3.03	11.18	7.45	9.42	3.69
CaO	1.22	5.39	5.04	11.91	0.02	1.24	7.65	4.54	0.00
Na_2O	6.90	0.03	0.06	7.59	1.09	6.71	0.03	0.01	0.50
K_2O	0.02	0.00	0.00	0.00	9.82	0.00	0.00	0.00	10.61
Total	98.77	99.72	99.27	100.00	95.90	97.58	99.84	99.09	95.63
Si	7.95	2.99	2.96	2.00	3.33	7.99	3.01	3.05	3.43
Ti	0.00	0.00	0.00	0.00	0.02	0.00	0.01	0.00	0.01
Al	1.69	1.94	1.94	0.42	2.25	1.70	1.93	1.97	2.09
Fe^{2+}	0.81	1.52	1.40	0.11	0.15	0.85	1.49	1.50	0.14
Fe^{3+}	0.25	0.08	0.15	0.09	0.00	0.19	0.04	0.00	0.00
Mn	0.01	0.04	0.03	0.00	0.00	0.00	0.03	0.02	0.00
Mg	2.29	0.98	1.09	0.39	0.30	2.27	0.86	1.08	0.37
Ca	0.18	0.44	0.41	0.45	0.00	0.18	0.63	0.37	0.00
Na	1.80	0.00	0.00	0.52	0.14	1.77	0.00	0.00	0.07
K	0.00	0.00	0.00	0.00	0.83	0.00	0.00	0.00	0.90
Total	14.98	7.99	7.99	4.00	7.01	14.95	8.00	8.00	7.00

[a] All Fe as FeO.

7. *P–T*-estimations

The $P-T$ calculations for the eclogite samples (Table 6) were based on the garnet–clinopyroxene geothermometer of Ellis and Green (1979), the garnet–phengite geothermometer of Green and Hellman (1982), and the garnet–clinopyroxene–phengite geobarometer of Waters and Martin (1993).

It is decisive for successful thermobarometry to choose mineral compositions that most probably represent equilibrium conditions. Chemical zonation in the analyzed garnet grains shows at least two zones: garnet cores low in pyrope, but high in grossular component and garnet rims with increased pyrope and decreased grossular contents, apparently, corresponding to the peak of metamorphism. Inasmuch as the recognition of truly coexisting zones of these three minerals involves difficulties, we correlate only cores of garnet and omphacite grains and the outermost garnet rims with the immediately contacting matrix omphacites and external zones of phengites.

The obtained results (Table 6) show enormous scatter of the calculated $P-T$ estimates. Possible reasons for such inconsistence and prominent examples were discussed recently by Schulte and Blümel (1999) and Nowlan et al. (2000). Among them, the following items may be considered: (a) uncertainties during correlation of mineral zones; (b) a partial disequilibration between minerals of eclogites during their multistage metamorphic history; (c) large analytical errors due to unknown ferric iron content in the minerals which influences distribution coefficients; and (d) secondary changes of coexisting mineral compositions (diffusion processes in zonal minerals, partial removal of the outermost zones, replacement by new minerals, etc.).

Despite the data scatter, some conclusions can be made: (1) The garnet–clinopyroxene temperatures show steadily higher values for garnet rims in comparison with garnet cores, indicating progressive metamorphism during growing of garnet grains. (2) The temperature estimates for the peak metamorphism as indicated by the garnet rims range from 640 to 790 °C with the calibration of Ellis and Green (1979). (3) The temperatures estimated using the garnet–phengite thermometer (560–720 °C) are not consistent with those of the garnet–omphacite geothermometer and are systematically lower. (4) It is evident that the pressure estimates obtained using the garnet–omphacite–phengite geobarometer of Waters and

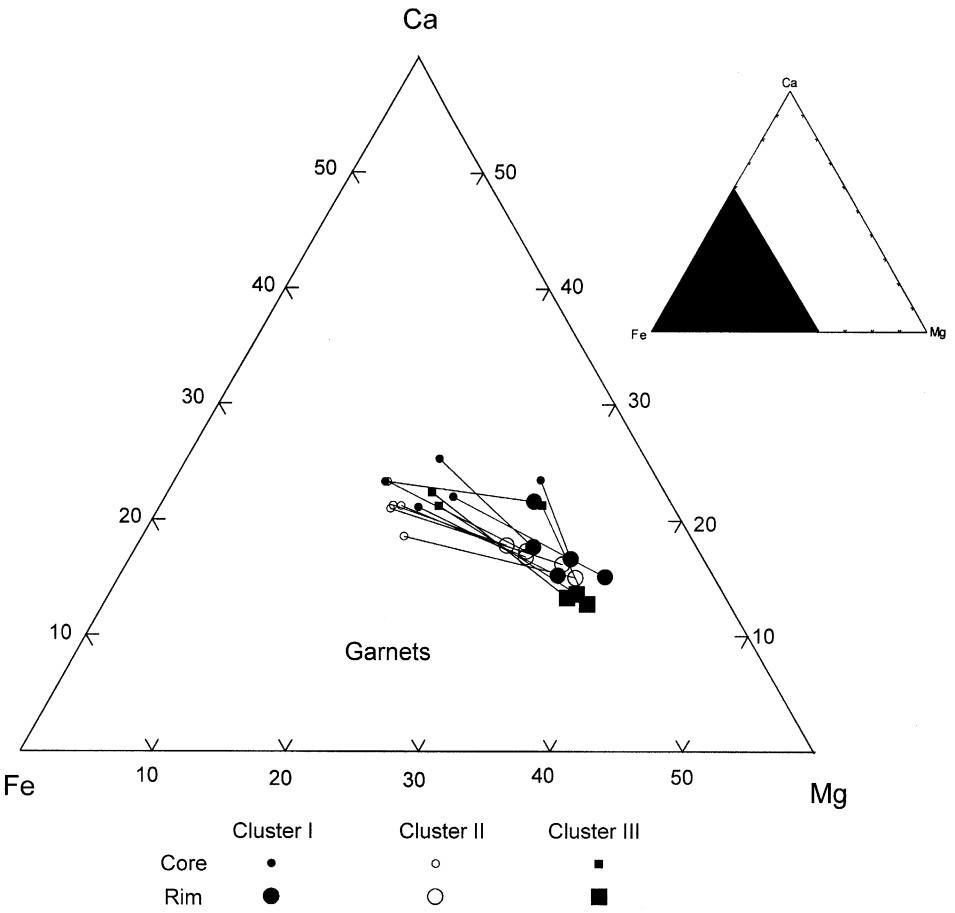

Fig. 6. Compositional range of garnets from the eclogites of the Maksyutov Complex.

Martin (1993) differ appreciably. The possible explanations for this unrealistic pressure scatter are discussed above. The main factor is considered to be a deviation of the actual mineral compositions from equilibrium ones due to different diffusion coefficients of chemical components in garnet, omphacite and phengite. Nevertheless, the obtained pressure values are consistent with the eclogite stability, but are contradictory to appearance of coesite. Based on the data on isotopic systematics, microtextures, and mineral zoning patterns, Glodny et al. (2002) concluded also that a pre-375 Ma stage of UHP metamorphism in the Maksyutov Complex can be ruled out.

Attempts to calculate the P–T conditions of metamorphism using the THERMOCALC program (Holland and Powell, 1998) led to similar results, reflecting a temperature increase and a pressure decrease during garnet growth and showing the considerable scatter of the P–T estimates. For example, the calculated P–T conditions for sample 21/1 are estimated to be the following: (a) 657 ± 46 °C, 22.2 ± 2.7 kbar (cores) and 749 ± 56 °C, 20.4 ± 3.1 kbar (rims) at $a_{H_2O} = 1.0$; (b) 638 ± 43 °C, 21.9 ± 2.7 kbar (cores) and 723 ± 51 °C, 19.9 ± 3.1 kbar at $a_{H_2O} = 0.5$.

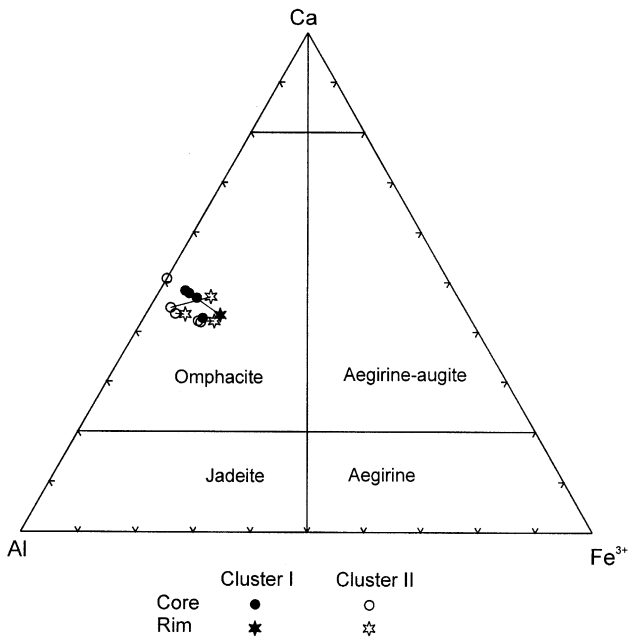

Fig. 7. Compositional range of clinopyroxenes in the examined eclogites.

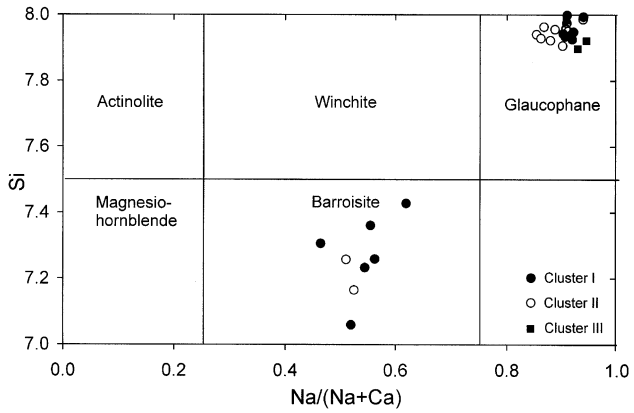

Fig. 8. Compositions of amphiboles plotted in terms of Si vs. Na/(Na + Ca) per formula unit.

8. Conclusions

1. The obtained data on major-oxide and trace-element chemistry of eclogites from the Maksyutov Complex suggests that their protoliths were quartz-bearing hypersthene-normative tholeiitic basalts.
2. The regular variations of the contents of major oxides and some incompatible trace elements suggest that the processes of fractional crystallization played an important role in formation of their protoliths. This conclusion is in agreement with the results obtained earlier by Leech and Ernst (2000). The established geochemical discrimination of eclogites of the Maksyutov Complex could be a result of fractional crystallization of basalt melt at shallow depths, which is supported by the presence of cumulative rocks. Therefore, the eclogitization was preceded by a crustal evolution of initial magmatic source, which is responsible for co-existence of rocks of variable composition in the same boudin. Dikes or sills of tholeiite basalts having geochemical characteristics of E-MORB could be protoliths for the considered eclogites.
3. The metamorphic processes have not affected greatly the major- and trace element signatures of initial rocks. Chemical compositions of co-existing minerals from the distinguished clusters do not show any significant distinctions. The scatter of the P–T estimates of metamorphic conditions is rather considerable, but not depends on whole-rock composition.

In summary it should be said that boudins, lenses and tectonic blocks of basic and ultrabasic rocks within the Lower Unit of the Maksyutov Complex are characterized by the great diversity of mineral and chemical composition. Therefore, the obtained results and our conclusions cannot be attributed to all eclogite bodies of this complex, as they could be the products of crystallization of different melts intruded in thinned continental crust shortly before subduction.

Table 6
Results of P–T calculations for eclogites of the Maksyutov Complex

Sample no.	Rock	Grt	Fe^{2+}/Mg (Grt)	Fe^{2+}/Mg (Cpx)	T (EG)	T (GH)	P (WM)
Cluster I							
8	Eclogite	Core	2.94	–	–		
		Rim	1.76	–	–	556	–
21/1	Eclogite	Core	2.09	0.24	699		
		Rim	1.51	0.24	731	647	22.7
21/2	Gln eclogite	Core	3.85	–	–		
		Rim	1.80	–	–	582	–
Cluster II							
10	Gln eclogite	Core	3.39	–	–		
		Rim	1.64	–	–	605	–
23/1	Gln eclogite	Core	3.32	0.36	673		
		Rim	1.91	0.36	790	630	21.6
23/2	Gln eclogite	Core	3.36	0.20	549		
		Rim	1.79	0.20	642	634	21.1
32/1	Gln eclogite	Core	1.55	0.47	752		
		Rim	1.46	0.28	753	716	15.5
		Core	1.67	0.35	669		
		Rim	1.74	0.22	674	682	15.0
Cluster III							
32/2	Eclogite	Core	2.92	–	–		
		Rim	1.50	–	–	706	–
		Core	1.74	–	–		
		Rim	1.39	–	–	659	–

The data for samples 32/1 and 32/2 include determinations for different mineral grains; EG = the garnet–clinopyroxene thermometer by Ellis and Green (1979); GH = the garnet–phengite thermometer by Green and Hellman (1982); WM = the garnet–omphacite–phengite barometer by Waters and Martin (1993).

Acknowledgements

We thank L.D. Kholodova and E.N. Nigmatulina for XRF and microprobe analyses. Our grateful thanks go to all the participants of the Third Workshop IGCP-420 for critical comments and fruitful discussion. We are most grateful to M. Leech and anonymous reviewer for critical and constructive reviews of the manuscript. B.M. Jahn is thanked for editorial comments. Financial support was given by the Russian Fund for Fundamental Research (N 02-05-64622 and N 00-05-65203).

References

Beane, R.J., Connely, J.N., 2000. $^{40}Ar/^{39}Ar$, U–Pb, and Sm–Nd constraints on the timing of metamorphic events in the Maksyutov Complex, southern Ural Mountains. Journal of the Geological Society, London 157, 811–822.

Beane, R.J., Liou, J.G., Coleman, R.G., Leech, M.L., 1995. Petrology and retrograde $P–T$ path for eclogites of the Maksyutov Complex, Southern Ural Mountains, Russia. The Island Arc 4, 254–266.

Brown, D., Spadea, P., 1999. Processes of forearc and accretionary complex formation during arc-continent collision in the southern Ural Mountains. Geology 27, 649–652.

Brown, D., Juhlin, C., Alvarez-Marron, J., Pérez-Estaun, A., Oslianski, A., 1998. Crustal-scale structure and evolution of an arc-continent collision zone in the southern Urals, Russia. Tectonics 17, 158–171.

Brown, D., Hetzel, R., Scarrow, J.H., 2000. Tracking arc-continent collision subduction zone processes from high-pressure rocks in the southern Urals. Journal of the Geological Society, London 157, 901–904.

Chemenda, A., Matte, P., Sokolov, V., 1997. A model of Palaeozoic obduction and exhumation of high-pressure/low-temperature rocks in the southern Urals. Tectonophysics 276, 217–227.

Chesnokov, B.V., Popov, V.A., 1965. Increasing volume of quartz grains in eclogites of the South Urals. Doklady AN SSSR 162, 909–910 (in Russian).

Dobretsov, N.L., 1974. Glaucophane schists and eclogite–blueschists complexes in the USSR, Nauka, Novosibirsk p. 430 (in Russian).

Dobretsov, N.L., 1991. Blueschists and eclogites: a possible plate tectonic mechanism for their emplacement from the upper mantle. Tectonophysics 186, 253–268.

Dobretsov, N.L., Dobretsova, L.V., 1988. New data on mineralogy of the Maksyutov eclogite–glaucophane schist complex. Doklady AN SSSR 294, 375–380 (in Russian).

Dobretsov, N.L., Shatsky, V.S., Coleman, R.G., Lennykh, V.I., Valizer, P.M., Liou, J., Zhang, R., Beane, R.J., 1996. Tectonic setting and petrology of ultrahigh-pressure metamorphic rocks in the Maksyutov Complex, Ural Mountains, Russia. International Geological Review 38, 136–160.

Echtler, H.P., Hetzel, R., 1997. Main Uralian Thrust and Main Uralian Normal Fault: non-extensional Palaeozoic high-P rock exhumation, oblique collision, and normal faulting in the Southern Urals. Terra Nova 9, 158–162.

Ellis, D., Green, D., 1979. An experimental study of the effect of Ca upon garnet–clinopyroxene Fe–Mg exchange equilibria. Contributions to Mineralogy and Petrology 71, 13–32.

Ernst, W.G., 1979. Coexisting sodic and calcic amphiboles from high-pressure metamorphic belts and the stability of barroisitic amphibole. Mineralogical Magazine 43, 269–278.

Glodny, J., Bingen, B., Austrheim, H., Molina, J.F., Rusin, A., 2002. Precise eclogitization ages deduced from Rb/Sr mineral systematics: the Maksyutov Complex, Southern Urals, Russia. Geochimica Cosmochimica Acta 66, 1221–1235.

Green, T.H., Hellman, P.L., 1982. Fe–Mg partitioning between coexisting garnet and phengite at high pressure, and comments on a garnet–phengite geothermometer. Lithos 15, 253–266.

Hetzel, R., 1999. Geology and geodynamic evolution of the high-P/low-T Maksyutov Complex, southern Urals, Russia. Geologische Rundshau 87, 577–588.

Hetzel, R., Echtler, H.P., Seifert, W., Schulte, B.A., Ivanov, K.S., 1998. Subduction- and exhumation-related fabrics in the Paleozoic high-pressure–low-temperature Maksyutov Complex, Antingan area, southern Urals, Russia. Bulletin of the Geological Society of America 110, 916–930.

Holland, T.J.B., Powell, R., 1998. An internally consistent thermodynamic data set for phases of petrological interest. Journal of Metamorphic Geology 16, 309–343.

Krasnobaev, A.A., Lennykh, V.I., Davydov, V.A., 1998. Geochronological evolution of the Maksyutov Complex (the Urals). Doklady RAN 362, 397–401 (in Russian).

Leech, M.L., Ernst, W.G., 1998. Graphite pseudomorphs after diamond? A carbon isotope and spectroscopic study of graphite cuboids from the Maksyutov Complex, south Ural Mountains, Russia. Geochimica et Cosmochimica Acta 62, 2143–2154.

Leech, M.L., Ernst, W.G., 2000. Petrotectonic evolution of the high- to ultrahigh-pressure Maksyutov Complex, Karayanova area, south Ural Mountains: structural and oxygen isotope constraints. Lithos 52, 235–252.

Lennykh, V.I., 1977. Eclogite–glaucophane schist belt in the South Urals, Nauka, Moscow p. 160 (in Russian).

Lennykh, V.I., Valizer, P.M., Beane, R.J., Leech, M.L., Ernst, W.G., 1995. Petrotectonic evolution of the Maksyutov Complex, Southern Urals, Russia: implications for ultrahigh-pressure metamorphism. International Geology Review 37, 584–600.

Matte, P., Maluski, H., Nicolas, A., Kepezhinskas, P., Sobolev, S., 1993. Geodynamic model and $^{39}Ar/^{40}Ar$ dating for generation and emplacement of the high pressure metamorphic rocks in SW Urals. Comptes Rendus de l' Academie des Sciences, Series 2, Mecanique, Physique, Chimie, Sciences de l' Univers, Sciences de la Terre 317, 1667–1674.

Meschede, M., 1986. A method of discriminating between different types of mid-ocean ridge basalts and continental tholeiites with the Nb–Zr–Y diagram. Chemical Geology 56, 207–218.

Mottana, A., Bocchio, R., Liborio, G., Morten, L., Maresch, V., 1985. The eclogite-bearing metabasaltic sequence of Isla Margarita, Venezuela: a geochemical study. Chemical Geology 50, 351–368.

Nowlan, E.U., Schert, H.-P., Schreyer, W., 2000. Garnet–omphacite–phengite thermobarometry of eclogites from the coesite-bearing unit of the southern Dora-Maira Massif, Western Alps. Lithos 52, 197–214.

Pearce, J.A., Cann, J.R., 1973. Tectonic setting of basic volcanic rocks determining using trace element analyses. Earth and Planetary Science Letters 19, 290–300.

Pearce, J.A., Norry, M.J., 1979. Petrogenetic implications of Ti, Zr, Y and Nb variations in volcanic rocks. Contributions to Mineralogy and Petrology 69, 33–47.

Piboule, M., Briand, B., 1985. Geochemistry of eclogites and associated rocks of the southeastern area of the French Massif Central: origin of the protoliths. Chemical Geology 50, 189–199.

Puchkov, V.N., 1997. Structure and geodynamics of the Uralian orogen. In: Burg, J.-P., Ford, M. (Eds.), Orogeny through time, Geological Society Special Publication, No. 121, pp. 201–236.

Shatsky, V.S., Jagoutz, E., Kozmenko, O.A., 1997. Sm–Nd dating of high-pressure metamorphism of the Maksyutov Complex, South Urals. Transactions of the Russian Academy of Sciences. Earth Science Section 353, 285–288.

Schulte, B.A., Blümel, P., 1999. Metamorphic evolution of eclogite and associated garnet–mica schist in the high-pressure metamorphic

Maksyutov complex, Ural, Russia. Geologische Rundschau 87, 561–576.

Schulte, B., Sindern, S., 2002. K-rich fluid metasomatism at high-pressure metamorphic conditions: lawsonite decomposition in rodingitized ultramafite of the Maksyutovo Complex, Southern Urals (Russia). Journal of Metamorphic Geology 20, 529–541.

Thompson, G., Bryan, W.B., Humphris, S.E., 1989. Axial volcanism on the East Pacific Rise, 10–12°N. In: Saunders, A.D., Norry, M.J. (Eds.), Magmatism in the Ocean Basins, Geological Society of London Special Publication 4, pp. 181–200.

Volkova, N.I., Frenkel, A.E., Budanov, V.I., Kholodova, L.D., Lepezin, G.G., 2001. Eclogites of the Maksyutov Complex, Southern Urals: geochemistry and the nature of the protolith. Geochemistry International 39, 935–946.

Wang, X., 1998. Metamorphic evolution of eclogite facies rocks in Northern Hubei and Southern Henan, China. Chinese Journal of Geochemistry 17, 5858–5868.

Waters, D.J., Martin, H.N., 1993. Geobarometry in phengite-bearing eclogites. Terra Abstracts 5, 410–411.

Winchester, J.A., Floyd, P.A., 1976. Geochemical magma type discrimination: application to altered and metamorphosed basic igneous rocks. Earth and Planetary Science Letters 28, 459–469.

Wood, D.A., 1980. The application of a Th–Hf–Ta diagram to problems of tectono-magmatic classification and establishing the nature of crustal containing of basaltic lavas of the British tertiary volcanic province. Earth and Planetary Science Letters 50, 11–30.

Xiao, Y.L., Hoefs, J., Van Den Kerkhof, A.M., Li, S.G., 2001. Geochemical constraints of the eclogite and granulite facies metamorphism as recognized in the Raobazhai complex from North Dabie Shan, China. Journal of Metamorphic Geology 19, 3–19.

Zhang, Z.M., Xu, Z., Xu, H., 2000. Petrology of ultrahigh-pressure eclogites from the ZK703 drillhole in the Donghai, eastern China. Lithos 52, 35–50.